Food Production, Processing and Nutrition

RESEARCH Open Access

Effects of freeze-thaw cycles on physicochemical properties and structure of cooked crayfish (*Procambarus clarkii*)

Jiping Han[1,2,3], Yingjie Sun[1,2,3], Rongxue Sun[1,3], Tao Zhang[4], Cheng Wang[1,3] and Ning Jiang[1,2,3*]

Abstract

To explore the damage mechanisms of freeze-thaw cycles on cooked crayfish in frozen storage, changes in the physicochemical properties and structure of cooked crayfish during the freeze-thaw cycles were investigated. The physicochemical properties of cooked crayfish changed significantly after five freeze-thaw cycles. The moisture content, water holding capacity, pH, and textural properties were decreased, while the total color difference, drip loss, and protein and lipid oxidation were significantly increased ($P < 0.05$). LF-NMR and MRI verified the water loss, and SDS-PAGE showed denaturation/degradation of myofibrillar proteins (MPs). Multiple freeze-thaw cycles promoted the transition from α-helix to β-turn in the secondary structure, the unfolding of tertiary structure, and a significant change in the chemical forces of MPs. SEM results revealed a disruption in the microstructure of muscle fibers. Repeated freeze-thaw cycles reduced the moisture content and distorted the structure of MPs in cooked crayfish, resulting in the disruption of physicochemical properties and its structure.

Keywords: Crayfish, Freeze-thaw cycles, Myofibrillar proteins, Structure

*Correspondence: jaas_jiangning@163.com

[3] Integrated Scientific Research Base for Preservation, Storage and Processing Technology of Aquatic Products of the Ministry of Agriculture and Rural Areas, Nanjing, People's Republic of China
Full list of author information is available at the end of the article

Graphical Abstract

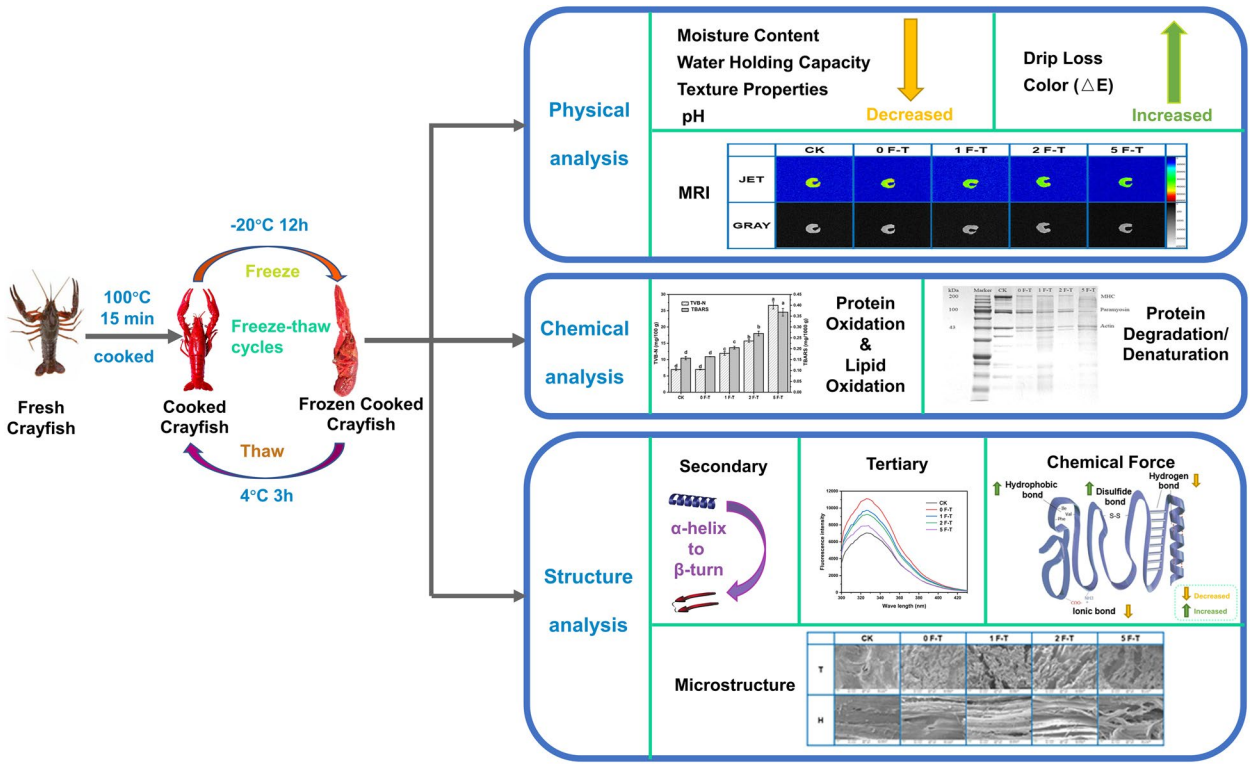

Introduction

Crayfish (*Procambarus clarkii*) is one of the most popular and important seafood in China with considerable economic significance (Pan et al. 2020). In recent years, the production and consumption of crayfish in China has rapidly developed. According to the Chinese Ministry of Agriculture, the annual turnover of the crayfish industry for the year 2020 was approximately RMB 344.846 billion. However, as a result of the Covid pandemic, e-commerce has gained complete control of the logistics of crayfish, catering to its consumption worldwide. Frozen cooked crayfish are selling like hotcakes on the Internet, with the overall market price continuing to climb year-on-year. Crayfish are favored by consumers for their unique flavor, rich protein, vitamin B, minerals, and low-fat content (Felix et al. 2017; Shi et al. 2020; Xu et al. 2022). However, similar to other fishery products, crayfish are susceptible to spoilage during transportation and storage due to three destructive mechanisms (microbial activity, chemical oxidation, and enzymatic reactions), making their storage and preservation crucial in the aquaculture processing industry (Sun, Chen, et al. 2019).

Freezing is a highly cost-effective method, not only extending the shelf life of seafood products but also maintaining their quality (Li et al. 2020; Wang et al. 2020). Therefore, freezing is currently one of the most commonly used methods for the storing, transporting, and preserving of seafood products (Leygonie et al. 2012; Wang et al. 2020). Freezing inhibits the microbial growth and enzymatic reactions in crayfish, while maximizing the retention of its original flavor and reducing the loss of nutrients during storage. Therefore, freezing is one of the conventional preservation techniques for extending the shelf life of crayfish, and retaining its original characteristics to the maximum level after thawing (Wang et al. 2020). Nevertheless, the concentration effect induced by freezing may result in the denaturation, segregation, and aggregation of proteins, since the effect alters the surface hydrophobicity of proteins. Besides, freezing can also increase the intramolecular and intermolecular disulfide bond exchange reactions, potentially changing the functional properties of proteins (Duan et al. 2017; Guo et al. 2015). Thus, the long-term freezing inevitably leads to ice crystal growth and protein denaturation, resulting in the deterioration of edible qualities

of seafood products, such as texture, water holding capacity (WHC), and color. This ultimately affects their sensory experience and commercial value to consumers.

In addition, temperature fluctuations during the transportation and circulation of frozen seafood products can cause multiple freeze–thaw cycles, and thawing is an important procedure for frozen products before further processing. Therefore, repeated freeze-thawing cycles are inevitable during processing of this kind of products (Frelka et al. 2019). Wang et al. (2021) showed that repeated freeze-thawing of pork patties increased the size of ice crystals and muscle damage due to temperature fluctuations, and that exposure of the side-chain groups of the protein amino acid residues led to a decrease in the sulfhydryl and free amino acid contents and an increase in the carbonyl content, which accelerated both protein and lipid oxidation. Ali et al. (2015) studied the effect of freeze-thaw cycles on protein stability in chicken breast and its relationship with lipid and protein oxidation; they discovered that multiple freeze-thaw cycles led to structural changes of the muscle fibers. The cryoprotective role of ice structuring proteins in mirror carp was reported by Du et al. (2021). They observed that samples to which ice structuring proteins were not added showed significantly reduced whiteness, water storage capacity, shear and thermal stability, and oxidation degree after repeated freeze-thawing. Wachirasiri et al. (2019) investigated the thawing losses and physical changes in mirror carp after multiple freeze-thaw cycles with non-phosphate additives. Repeated freeze-thawing resulted in thawing losses that led to a decrease in the WHC, thiobarbituric acid value, and salt-soluble protein content, and shear force. However, limited studies focused on the effects of freeze-thaw cycles on the physicochemical properties and structure of cooked seafoods, particularly in crayfish.

This study aimed to investigate the quality differences on cooked crayfish after repeated freeze-thaw cycles and to obtain the key factors affecting the quality of cooked crayfish. First, the changes in the WHC, drip loss, texture characteristics, color, water status and distribution, the lipid and protein oxidation were evaluated. Then, the secondary and tertiary structures of myofibrillar proteins as well as the chemical forces was investigated. Moreover, the microstructure of muscle fibers in cooked crayfish was also clarified. The results can provide theoretical supports for the quality enhancement of cooked crayfish during frozen storage.

Materials and methods

Materials and reagents

Fresh crayfish (*P. clarkii*) were obtained from a local supermarket in Nanjing, China. The 2× sodium dodecyl sulfate-polyacrylamide gel electrophoresis (SDS-PAGE) loading buffer, precast gel HEPES SDS- 12% PAGE (10-well), and RealBand 3-color regular range protein marker (5–245 kDa) were obtained from Sangon (Sangon Biotech [Shanghai] Co., Ltd., Shanghai, China). Other reagents and chemicals were of analytical grade and purchased from Sinopharm Group Co., Ltd.

Sample treatment

Fresh crayfish weighing 25 ± 2 g were selected for the experiment. All the samples were washed under running water to remove sediment from the surface. The shelled fresh crayfish without any treatments were used as the control, named as CK. The crayfish were cooked at 100 °C for 15 min while stirring intermittently for four times. The shells were removed, and the meat was drained for 30 min to remove water from the surface. The samples were then randomly divided into four groups. They were analyzed and characterized after 0, 1, 2, and 5 freeze-thaw cycles, named 0 F-T, 1 F-T, 2 F-T, and 5 F-T, respectively. One freeze-thaw cycle comprised storing the crayfish at − 20 °C for 12 h and thawing it at 4 °C for 3 h.

Low-field nuclear magnetic resonance (LF-NMR) and magnetic resonance imaging (MRI) measurements

A MesoMR23-060H-I NMR Imaging and Analyzing system (Suzhou Niumag Analytical Instrument Co., Ltd., Suzhou, China) was conducted to estimate the dynamic moisture content and water state of cooked crayfish after the freeze-thaw cycles. The LF-NMR analysis was performed using a pretreatment magnet of field strength 0.47 T and a proton resonance frequency of 20 MHz, at a temperature of 32 °C. The samples were placed in a glass tube with an outer diameter of 60 mm and were inserted into the NMR probe. The water transverse (or spin–spin) relaxation time (T_2) was measured based on the Carr–Purcell–Meiboom–Gill (CPMG) pulse sequences. The test settings were as follows: a 14 μs wide 90° pulse, a 26.48 μs 180° wide pulse, time waiting (TW) 3500 ms, repeated scanning number (NS) 16, number of echo count (NECH) 15,000, and echo time (TE) 200 μs.

The hydrogen proton density and distribution in crayfish were determined using MRI. The MRI parameters were as follows: echo time (TE), 20 ms; repetition time (TR), 500 ms; read size × phase size, 256 × 192; average number, 4; and field of view (FOV), 100 × 100 mm. Each experiment was repeated at least three times.

Measurement of physicochemical properties

Measurement of moisture content

The gravimetric technique was used to determine the moisture content of cooked crayfish samples (Sinha & Bhargav 2020).

Measurement of water holding capability (WHC)

The WHC of crayfish was measured according to the method described by Zhuang et al. (2021). About 2-g crayfish was wrapped in absorbent cotton and deposited in a 50-mL centrifuge tube for 10 min (9000 r/min, 4 °C). The experiment was repeated three times independently. WHC was calculated using the following equation:

$$\mathrm{WHC}\ (\%) = \left(1 - \frac{m_1 - m_2}{m_1}\right) \times 100 \quad (1)$$

where m_1 is the initial weight of crayfish, and m_2 is the weight of crayfish after centrifugation.

Measurement of drip loss (DL)

The DL values of cooked crayfish samples were determined according to the method described by Li et al. (2021). The cooked crayfish was weighed before thawing (m_3). After thawing, the surface of cooked crayfish was wiped with absorbent paper and weighed (m_4). DL was calculated using the following equation:

$$\mathrm{DL}\ (\%) = \frac{m_3 - m_4}{m_3} \times 100 \quad (2)$$

Color difference analysis

The color difference of the cooked crayfish samples was determined using a color meter (Shanghai Precision Instruments Co., Ltd., Shanghai, China) according to the method specified by Alizadeh-Sani et al. (2021). The surface water of the thawed cooked crayfish was removed using a filter paper, and the CIE-Lab L*, a*, and b* values were recorded. The total color difference (ΔE) was calculated using the following equation:

$$\Delta E = \sqrt{\left(L_0^* - L^*\right)^2 + \left(a_0^* - a^*\right)^2 + \left(b_0^* - b^*\right)^2} \quad (3)$$

where L_0^*, a_0^*, b_0^* and L*, a*, b* were the lightness, redness/greenness, and yellowness/blueness values of fresh cooked crayfish and freeze-thawed cooked crayfish, respectively.

Texture property analysis (TPA)

The texture properties (including hardness, springiness, and chewiness) of the cooked crayfish samples were measured using a texture analyzer (Brookfield Engineering Laboratories, Inc., Middleboro, MA, USA). The first and second ventral abdominal muscles of the cooked crayfish samples were selected for TPA, and the analysis was conducted using a TA11/1000 Cylinder probe (25.4 mm in diameter and 35 mm in length). All the samples should be cut into 1 cm × 1 cm × 0.8 cm. The test speed, deformation ratio, and trigger force were set as 1 mm/s, 50%, and 5 g, respectively (Xu et al. 2020).

Measurement of pH

The pH values of the cooked crayfish samples were measured using a digital pH meter (Mettler-Toledo Instruments Co., Ltd., Shanghai, China) at 4 °C. About 5 g cooked crayfish was homogenized in 45 mL distilled water using the IKA T18 digital ULTRA-TURRAX Homogenizer system (IKA Ltd., Germany) for 1 min (4 °C, 10,000 r/min). The pH value of the solution was measured using the digital pH meter (Ali et al. 2015).

Measurement of total volatile basic nitrogen (TVB-N)

The TVB-N content in the cooked crayfish samples was determined according to the method reported by Li et al. (2019), with minor modifications. About 3 ± 0.01 g sample was homogenized in 15 mL distilled water for 1 min (4 °C, 10,000 r/min). The sample mixture was filtered using a Whatman filter paper (Φ = 15 cm; Hangzhou Whatman-Xinhua Filter Paper Co., Ltd., China). The Conway method was used to measure the TVB-N values at 37 ± 1 °C for 2 h. After heating, the crayfish samples were transferred into an alkaline solution and subsequently soaked in a boric acid solution (20 g/L). The resulting distillate was combined with two or three drops of a mixed indicator, which consisted of 1 g/L methyl red in ethanol and 5 g/L bromocresol green. Conway was cooled it to room temperature and then titrated it with standard hydrochloric acid solution (0.0010 M) until the purple red end point was reached. The TVB-N values were calculated using the following equation:

$$\mathrm{TVB-N}\ (\mathrm{mg}/100\ \mathrm{g}) = \frac{0.001 \times 14 \times (V - V_0)}{m \times (1/15)} \times 100 \quad (4)$$

where m was the mass of the cooked crayfish, and V and V_0 were the volumes consumed of the standard hydrochloric acid solution and blank, respectively.

Measurement of thiobarbituric acid-reactive substances (TBARS)

The TBARS value in cooked crayfish was measured according to the method described by Jiang et al. (2019). The cooked crayfish samples were homogenized in a solution containing trichloroacetic acid-hydrochloride (TCA-HCl) and ethylenebis (oxyethylenenitrilo) tetraacetic acid (EGTA) for 1 min (10,000 r/min) and shook for 30 min (50 °C). After filtration, the filtrate was mixed with 5 mL TBA (0.02 M) solution. The solution was then incubated in water (90 °C, 40 min), cooled to room temperature, and the absorbance was determined

at 532 nm using a UV–VIS spectrophotometer (UV-6300; Mapada Instruments, Shanghai, China); 5 mL distilled water was used as the blank instead of the filtrate. The absorbance was compared with the standard curve of malondialdehyde (MDA). The values of TBARS were expressed as mg/1000 g of the crayfish sample.

Extraction of myofibrillar proteins (MPs)

MPs were extracted from cooked crayfish samples according to the method described by Shi et al. (2021). The extracted MPs were then dissolved in phosphate-buffered saline (0.6 M KCl, 10 mM K_2HPO_4, pH 6.0) and were utilized within 3 days. The protein concentration was determined using the biuret method with bovine serum albumin as the standard. The standard curve was $y = 0.0244x - 0.0044$, $R^2 = 0.9996$.

Sodium dodecyl sulfate-polyacrylamide gel electrophoresis (SDS-PAGE)

SDS-PAGE was conducted to determine the structural changes in MPs (Hu, Qian, et al. 2021). Briefly, the protein concentration was adjusted to 1 mg/mL. The MPs were mixed with 2× loading buffer (Sangon Biotech [Shanghai] Co., Ltd., Shanghai, China) in a ratio of 1:1 (v/v). The mixture was then boiled for 10 min (95 °C) and centrifuged for 5 min (10,000 r/min). Following this, 20-μL supernatant and 10-μL marker were added into the loading well. The electrophoretic buffer (50 mM Tris, 50 mM HEPES, 0.1% SDS, 2 mM EDTA) was added and the electrophoresis was carried out at 150 V for 40 min. After electrophoresis, the gel was soaked for 4.5 h in a Coomassie brilliant blue R-250 dye solution containing 5% ethanol, 10% glacial acetic acid, and 85% distilled water for decolorization, until the protein bands could be identified. The Image Lab gel imaging system (Tanon 2500; Tanon Science & Technology, Co., Ltd., Shanghai, China) was used to analyze the electrophoretic gels.

Raman spectroscopy analysis

Laser Raman spectroscopy of cooked crayfish samples were performed using the Raman spectrometer (DXR532; Thermo Fisher Scientific, USA) according to the method described by Lan et al. (2021). A 785-nm argon laser ion source was used for excitation. Data were collected in the scanning range of 400–4000 cm^{-1} with a spectral resolution of 3 cm^{-1}. Peakfit 4.12 (SeaSolve Software, Inc., Framingham, MA, USA) was utilized to fit and analyze the secondary structure of the proteins in crayfish. The secondary structure of the proteins in cooked crayfish samples was determined and expressed as a percentage of α-helix, β-sheet, β-turn, and random coil conformation according to Yang et al. (2021).

Endogenous fluorescence spectra analysis

The intrinsic fluorescence intensities of the cooked crayfish samples were determined by fluorescence spectroscopy using the Cytation 3 Cell imaging multi-mode microplate reader (BioTek Instruments, Winooski, VT, USA). The concentration of the MPs was adjusted to 500 μg/mL. The MP solution was taken in opaque 96-well plates. The excitation wavelength was 280 nm, and the emission spectra ranged from 300 to 430 nm. The excitation and emission slit width was 2.5 nm, and the scanning speed was 2 nm/s.

Measurement of chemical forces

The chemical forces in the cooked crayfish samples were analyzed according to the method described by Li et al. (2021), with some modifications. Each cooked crayfish sample was mixed with a mixture containing solutions A (0.05 M NaCl), B (0.6 M NaCl), C (0.6 M NaCl + 1.5 M urea), D (0.6 M NaCl + 8 M urea), and E (0.6 M NaCl + 8 M urea + 0.5 M β-mercaptoethanol) in the ratio of 1:9 (w/v). The protein concentration in the supernatant was determined using the biuret method. The contents of the ionic, hydrogen, hydrophobic, and disulfide bonds were expressed as the difference in the protein concentrations dissolved in solutions A and B, B and C, C and D, and D and E, respectively.

Scanning electron microscopy (SEM)

The cooked crayfish samples were cut into pieces of dimension 5 mm × 5 mm × 5 mm and soaked in 2.5% glutaraldehyde solution overnight. The samples were then washed with 0.1-M phosphate buffer (pH 7.2) for 15 min; this step was repeated for four times. The samples were then dehydrated with 50, 70, 80, 90, and 100% ethanol solution for 10 min, respectively. Finally, the samples were dried using a freeze dryer. They were then placed on the sample table of the Zeiss EVO-LS10 scanning electron microscope (ZEISS, Oberkochen, Germany) with the observation surface upward. Ion sputtering and gold spraying were done using an ion sputter coater (Wang et al. 2021).

Statistical analysis

The experiments were conducted in three replicates. For repeated experiments, the results were expressed as mean and standard deviation. The data were analyzed by one-way analysis of variance (ANOVA), and the significant difference between the mean values was determined by Duncan's multiple range test ($p < 0.05$) using SPSS statistical software v. 19.0 (SPSS, Inc., Chicago, IL, USA).

Results and discussion

LF-NMR and MRI analyses of the freeze-thaw process

In order to investigate the effect of freeze-thaw cycles on the water distribution and dynamic water status change in cooked crayfish, the relaxation characteristics of cooked crayfish were determined using CPMG pulse sequences to obtain the transverse relaxation time (T_2). As illustrated in Fig. 1a, three peaks were observed for the cooked crayfish samples: T_{21} (1–10 ms), corresponding to the bound water, that is, the water that was tightly bound to the biomolecules; T_{22} (10–100 ms), corresponding to the immobile water, that is, the water in the myogenic fibrin network; and T_{23} (100–1000 ms), corresponding to the free water, that is, the water outside the MP network and has a direct impact on DL and WHC (Chen, Li, et al. 2020). After five freeze-thaw cycles, the T_{22} of cooked crayfish was found to be reduced by 14.7% when compared with that of CK ($p < 0.05$), demonstrating that the immobilized water was converted to another state of water during repeated freeze-thaw process. The disruption in cell integrity and muscle fiber contraction made part of T_{22} to migrate out of the cell, and also aggravated the release and transformation of immobile water in the muscle tissue to a certain extent. In the process of repeated freezing-thawing, ice crystals could be formed in different sizes and positions during each freezing-thawing cycle. The shifted sizes and positions of the ice crystals were found to destroy the cells and myofibrillar proteins, resulting in a destruction on the structures of muscle proteins. Besides, the freeze-thaw cycles also reduced the macromolecules in the side chains of proteins that can bind with water molecules, therefore enhancing the release and transformation of the immobile water in muscle tissues. In addition, the loss in moisture content was found to be strongly connected to the degradation of cell membranes and MPs induced by recurrent ice crystal formation, particularly after four cycles (Tan et al. 2018).

The ^{1}H MRI proton density-weighted imaging pseudocolor map of crayfish flesh corresponding to the increasing number of freeze-thaw cycles was shown in Fig. 1b. The pseudocolor image tended to be red, suggesting a strong water proton signal, that is, a high moisture content in this part. As the number of freeze-thaw cycles increased, the brightness of the pseudocolor image was found to decrease gradually. The change in brightness was more obvious after repeated freeze-thaw cycles. The pseudocolor image gradually tended to the background color, indicating that repeated freeze-thaw cycles intensified the water loss in cooked crayfish. Lan et al. (2020) have found that repeated freeze-thaw cycles potentially caused water to be constantly transported from the intracellular to the extracellular areas, resulting in perimysium leakage or alteration in certain protein conformations. The changes further resulted in an increase in the free water content and DL, indicating the worse water loss in cooked crayfish.

Analysis of physical properties

The WHC and DL of meat could affect the nutrient content, tenderness, color, and other qualities of crayfish, which are important indicators in meat quality assessment. The effects of freeze–thaw cycles on the WHC and DL of cooked crayfish are shown in Table 1. During the multiple freeze-thaw process, the moisture content and WHC of cooked crayfish significantly decreased, while the DL was much higher than that of CK ($p < 0.05$). During the freeze-thaw process of cooked crayfish, the water in the muscle tissue was rearranged by the formation of ice crystal, resulting in a contraction of cells. Further, the mechanical damage induced by the ice crystals affected the entire tissue structure. During the initial thawing

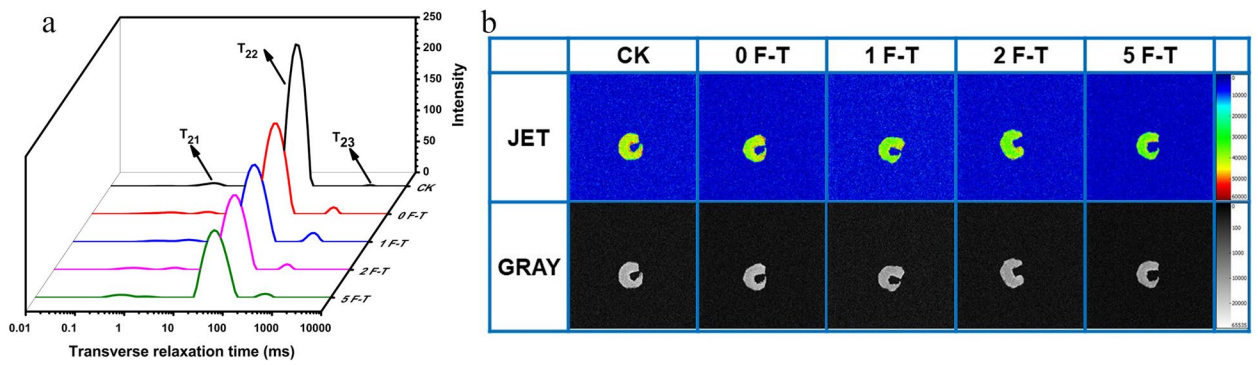

Fig. 1 Changes in transverse relaxation time (T_2) (**a**) and proton density images of cooked crayfish subjected to repeated freeze-thaw cycles (**b**) (CK: fresh crayfish; 0 F-T: cooked crayfish with 0 freeze-thaw cycle; 1 F-T: cooked crayfish with 1 freeze-thaw cycle; 2 F-T: cooked crayfish with 2 freeze-thaw cycles; 5 F-T: cooked crayfish with 5 freeze-thaw cycles)

Table 1 Effects of repeated freeze thaw cycles on the quality properties of cooked crayfish

Indicator	Moisture content (%)	WHC (%)	DL (%)	L*	a*	b*	ΔE	Hardness (g)	Springiness (mm)	Chewiness (mJ)	pH
CK	81.68 ± 0.56^{a}	83.86 ± 1.36^{a}	–	26.85 ± 0.40^{d}	0.81 ± 0.07^{e}	1.89 ± 0.06^{d}	–	744 ± 78^{c}	1.99 ± 0.11^{c}	5.92 ± 0.54^{d}	6.92 ± 0.19^{c}
0 F-T	79.48 ± 1.50^{b}	75.33 ± 4.48^{b}	–	27.66 ± 0.22^{cd}	2.73 ± 0.11^{a}	2.58 ± 0.09^{c}	2.46 ± 0.07^{d}	1569 ± 88^{a}	3.44 ± 0.16^{a}	33.79 ± 2.94^{a}	7.85 ± 0.04^{a}
1 F-T	79.27 ± 1.25^{b}	68.55 ± 3.07^{c}	13.39 ± 1.46^{b}	28.13 ± 0.20^{c}	2.28 ± 0.12^{b}	2.72 ± 0.08^{bc}	2.16 ± 0.05^{c}	1156 ± 106^{b}	3.39 ± 0.11^{a}	25.64 ± 3.11^{b}	7.78 ± 0.01^{a}
2 F-T	78.01 ± 0.88^{bc}	68.01 ± 2.82^{c}	15.05 ± 1.09^{b}	29.87 ± 0.44^{b}	1.98 ± 0.14^{c}	2.83 ± 0.28^{b}	3.34 ± 0.10^{b}	1029 ± 116^{b}	3.25 ± 0.26^{b}	23.08 ± 2.17^{b}	7.69 ± 0.12^{ab}
5 F-T	76.26 ± 1.61^{c}	66.30 ± 4.44^{c}	19.72 ± 1.60^{a}	31.92 ± 1.04^{a}	1.43 ± 0.13^{d}	3.19 ± 0.12^{a}	5.15 ± 0.13^{a}	934 ± 65^{c}	3.06 ± 0.14^{b}	16.98 ± 1.53^{c}	7.35 ± 0.37^{b}

L*, a*, and b* representedluminosity, redness and yellowness, respectively. Different letters in the same column of the same indicator showed significant difference ($p < 0.05$)

process, the muscle fibers could remain their structures and the water could be partly maintained after thawing. With repeated freeze-thaw cycles, this destructive effect intensified. Similarly, an increased DL value was discovered on the lightly salted tuna meat, when exposed to numerous freeze-thaw cycles (Jiang et al. 2019). It may be due to the damage of muscle fiber microstructures and protein solubilization.

Color was a significant parameter in evaluating the quality of cooked crayfish for consumers. The physicochemical quality of meat, particularly, their color and texture, was influenced by the freeze-thaw cycles (Zhou et al. 2021). The changes in the color of cooked crayfish throughout the freeze-thaw cycles are shown in Table 1. With multiple freeze-thaw cycles, the values of L* and b* increased significantly, while the value of a* decreased markedly ($p < 0.05$). Moreover, it should be noted that the total color difference (ΔE) values of the cooked crayfish samples were higher than that of CK after repeated freeze-thaw cycles ($p < 0.05$), indicating that the freeze-thaw cycles had a detrimental effect on the color stability of the cooked crayfish samples. The stability of meat color was deeply affected by the storage temperature. The structural damage of muscle fibers was exacerbated by temperature fluctuation during storage, resulting in an increased water loss of the muscle. Then large amounts of water leaking out and building up on the surface of muscle, leading to a deterioration in the color of the meat. A similar phenomenon was found in cuttlefish with several freeze–thaw cycles, where the increased lipid oxidation of cuttlefish was coincidental with an increase in b* values (Shi et al. 2021). Moreover, Sun et al. (2021) observed that after numerous freeze-thaw cycles, the DL and the oxidation of the pigmented proteins of carp were aggravated, which caused a decrease in the values of a* and b*.

The texture property can directly reflect the quality characteristics of meat. The results of the texture parameters of the cooked crayfish samples after multiple freeze-thaw cycles are shown in Table 1. As the increasing number of freeze-thaw cycles, a significant decrease was observed in the hardness, springiness, and chewiness of the cooked crayfish ($p < 0.05$). During repeated temperature fluctuations process, the ice crystals gradually increased in size and number in the frozen meat sample. It led to the increase of the DL on crayfish, resulting in a sharp decrease in its texture properties. Moreover, the worsening of texture properties was mainly caused by lipid oxidation, as repeated temperature fluctuations could promote lipid oxidation. It was observed that ice crystals caused mechanical damage to muscle cells during repeated freeze-thaw cycles, which leding to a sharp decrease in the texture properties and consumer acceptability of cooked crayfish (Hu, Zhang, et al. 2021).

The pH of meat is highly correlated with its color, WHC, tenderness, and other meat quality parameters (Alarcon-Rojo et al. 2019). No significant difference was observed in the pH values of cooked crayfish during the initial two freeze-thaw cycles ($P > 0.05$). However, the pH value decreased from 7.69 to 7.35 after five freeze-thaw cycles. The freezing process would start outside the cells, as water migrated from the inner muscle to the outside of muscle fibers. The dehydration and transverse shrinking of muscle fibers and MPs would be caused by the migration of water. Outside of the ice crystals, the solutes become more concentrated, leading to a higher content of protons, as a result, a reduction in the pH of crayfish sample. In addition, with multiple freeze-thaw cycles, the glycogenolysis was caused by the oxygen and microorganisms in the crayfish sample, which depleted the adenosine triphosphate in the sample, leading to a reduction in pH. As reported previously, thawing caused an increase in glycolysis and an activation of phosphatases, resulting in a lower pH (Sun et al. 2021).

Analysis of oxidation characteristics

TVB-N and TBARS were considered the indicators for assessing the oxidation characteristics of freeze-thaw cycles on cooked crayfish, as shown in Fig. 2a. For fresh crayfish, TVB-N value was 6.9417 ± 0.3086 mg/100 g and the TBARS value of was 0.1569 ± 0.0079 mg/1000 g. After repeated freeze-thaw cycles, the TBARS and TVB-N values of the cooked crayfish samples were 2.35 and 3.84 times higher, respectively, when compared with that of CK ($P < 0.05$).

Conventionally, TVB-N (mg/100 g) ≤ 20 mg/100 g are considered qualified products. After five freeze-thaw cycles, the TVB-N value was 26.6299 ± 1.1192 mg/100 g, which implied that the cooked crayfish was no longer suitable for consumption. The results clearly demonstrated that freeze-thaw cycles could intensify the oxidative degradation of the proteins in crayfish. Repeated freeze-thaw cycles further deteriorated the color and texture of cooked crayfish by reducing its moisture content and pH, resulting in a significant reduction in WHC and a significant increase in DL, thereby disrupted the internal structure of the meat, leading to the breakdown of MPs and nitrogenous compounds. According to Li et al. (2020), thawing may cause large amounts of nutrients to leak from the cells to the surface of salmon, and, ultimately, contribute to the accumulation of TVB-N.

Generally, the biochemical changes caused by oxidative stress are lipid peroxidation like that of MDA. Its accumulation could destroy the structure and functions of cells, thereby affecting the normal progress of a series of physiological and biochemical reactions. Based on the results, it was speculated that multiple freeze-thaw

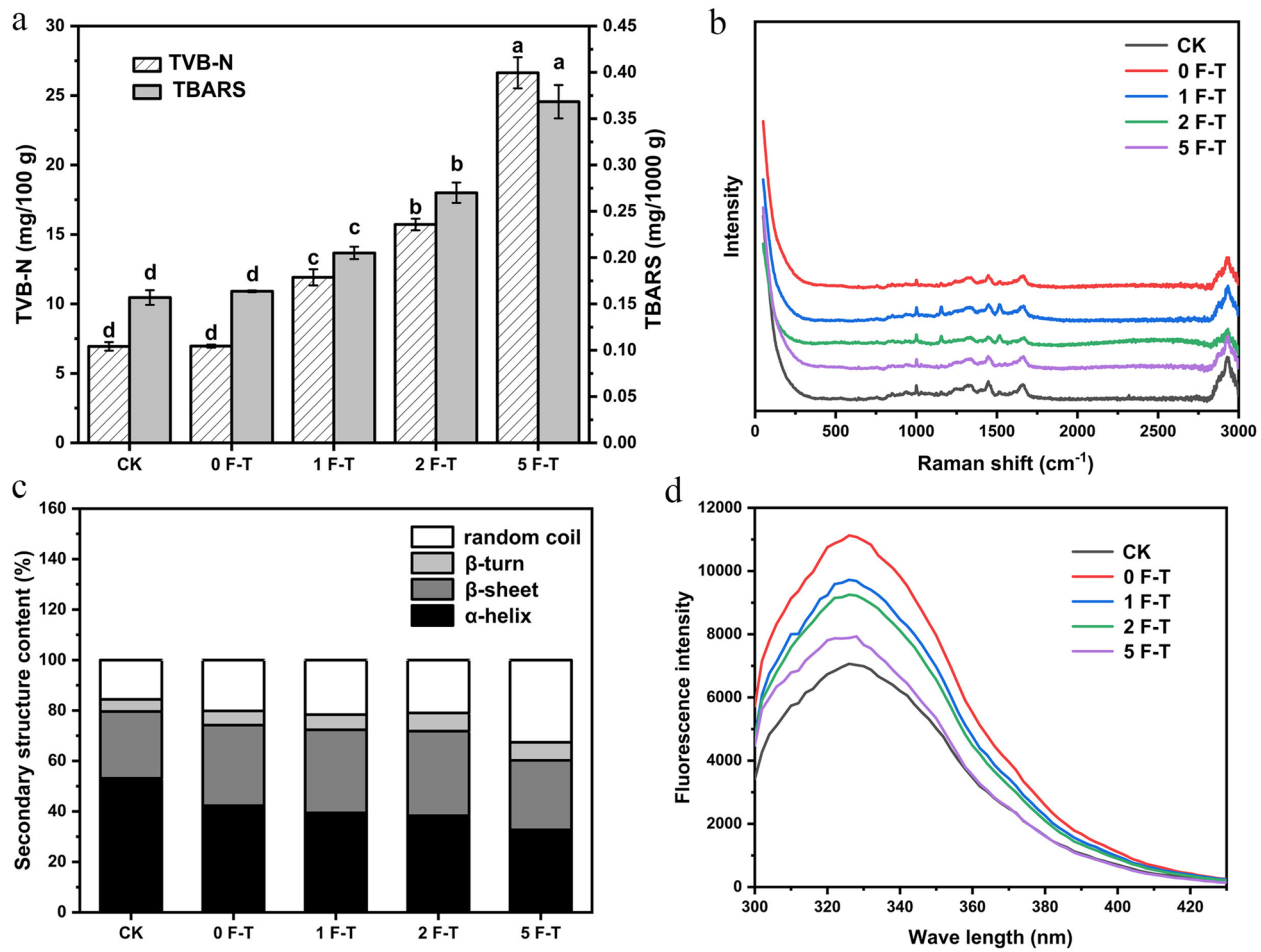

Fig. 2 Effect of repeated freeze thaw cycles on the TVB-N and TBARS values of cooked crayfish (**a**), Raman spectra of MPs of cooked crayfish during repeated freeze-thaw cycles (**b**), changes in the secondary structure of cooked crayfish after repeated freeze-thaw cycles (**c**), and endogenous fluorescence spectra of MPs after repeated freeze-thaw cycles (**d**) (CK: fresh crayfish; 0 F-T: cooked crayfish with 0 freeze-thaw cycles; 1 F-T: cooked crayfish with 1 freeze-thaw cycle; 2 F-T: cooked crayfish with 2 freeze-thaw cycles; 5 F-T: cooked crayfish with 5 freeze-thaw cycles). Different letters in the same column of the same indicator showed significant difference ($p < 0.05$)

cycles accelerated lipid oxidation, indicated by an increase of the TBARS value. Moreover, after repeated freeze-thaw, the ice crystals and recrystallisation were formatted, with large ice crystals causing cell damage of the muscle. Moreover, some oxidative enzymes flowing out with the drip loss, promoting the lipid oxidation. In this study, the exorbitant lipid oxidation led to a severe change in color and taste, and a steep fall in the quality of cooked crayfish, partially confirming the above conclusions.

Secondary and tertiary structures of MPs

The effects of multiple freeze-thaw cycles on the secondary structure of MPs were characterized by Raman spectroscopy. Figure 2b shows the Gaussian-fitted Raman spectra of the amide I band of MPs of cooked crayfish after multiple freeze-thaw cycles. In the figure, the peaks at the Raman shifts 1645–1660, 1665–1680, 1680–1690, and 1660–1670 cm^{-1} characterized the α-helix, β-sheet, β-turn, and random coil, respectively. After five freeze-thaw cycles, the percentage of α-helix was found to decrease significantly; however, the percentage of β-turn increased ($p < 0.05$) (Fig. 2c). The results implied that repeated freeze-thaw cycles destabilized the secondary structure of MPs in cooked crayfish, potentially causing the conversion of α-helix to β-turn. The α-helix was an important secondary structural unit with a certain degree of rigidity, which supported the overall conformation of MPs. Pan et al. (2021) also pointed out that the α-helix proportion decreased as the protein oxidation increased. In concordance with the current study, they observed that the lipid and protein oxidation were exacerbated due to multiply freeze-thaw cycles. In addition, Wang et al. (2021) confirmed that the protein oxidation

caused by the freeze-thaw cycles aggravated the decrease in the proportion of α-helix conformation, which was consistent with the TVB-N value above.

Endogenous fluorescence spectroscopy can explain the conformational changes in MPs due to the position and microenvironment of the aromatic amino acid residues. The endogenous fluorescence spectra of the MPs are shown in Fig. 2d. When compared with that of CK, the fluorescence intensities of the cooked crayfish MPs were significantly higher ($p < 0.05$). It implied that the high-temperature treatment denatured the MPs, exposing the tryptophan side-chain group from the internal hydrophobic region to the solvent and enhancing the fluorescence intensity. The result was in agreement with the earlier studies of Chen, Zhou, et al. (2020). After multiple freeze-thaw cycles, the fluorescence intensities of cooked crayfish MPs decreased from 11,123 to 7880 a.u. ($p < 0.05$), indicating that the natural structure of the MPs changed during the process of freeze-thaw. It has been observed that the unfolding of the structure of MPs, change in the internal hydrophobic environment, and the exposure of the tryptophan residues inside the MPs could decrease the fluorescence intensity. In consistent with the results of the present study, Pan et al. (2021) found that repeated freeze-thaw cycles partially unfolded the MPs from quick-frozen pork patties, resulting in a decrease of the fluorescence.

Analysis of chemical forces

The effects of the freeze-thaw cycles on chemical forces are shown in Fig. 3a–d (including ionic, hydrogen, hydrophobic, and disulfide bonds). The change in chemical force was an important factor affecting the texture characteristics of cooked crayfish. With the increasing number of freeze-thaw cycles, the solubility of the ionic and hydrogen decreased gradually, while that of the hydrophobic and disulfide bonds increased significantly ($p < 0.05$).

The structure of muscle proteins is maintained by chemical interactions such as ionic bonds, hydrogen bonds, disulfide bonds, and hydrophobic interactions. The changes in these chemical interactions have shown great effect on textural properties of muscle proteins. During freeze-thaw cycles, the chemical interactions are potentially disrupted, resulting in protein conformational changes. Compared with hydrophobic and disulfide bonds, the non-covalent bonds, e.g., ionic and hydrogen bonds, are weaker bonding forces, and therefore can be easily broken after multiple freeze-thaw cycles. It has been proved that the hydrogen bond was the main secondary bond to maintain the stability of α-helix. For instance, Wang et al. (2022) clarified that the decrease in the α-helix content indicated a breakdown of the intramolecular hydrogen bonds and an increase in protein molecular unfolding. Therefore, the decreased hydrogen bond content in the current study was consistent with the change of α-helix (Fig. 2c).

On the other hand, hydrophobic interactions and disulfide bonds are much more stable, playing a key role in the structure of cooked crayfish. However, the rapid increase in the number of hydrophobic and disulfide bonds could be associated with the lipid and protein oxidation, resulting in the denaturation and aggregation of muscle proteins (Shi et al. 2021). As reported previously, the formation of disulfide bonds may result in the loss of the sulfhydryl groups, which is one of the earliest observable events during the oxidation of proteins (Dean, Fu, Stocker, & Davies, 1997). Additionally, the formation of disulfide bonds in myofibrillar proteins may induce the occurrence of protein–protein cross-linked derivatives in meat, affecting its drop loss and tenderness. It was due to the fact that the mechanism of water-holding, in the form of binding and entrapping, relates to the physical structures of the myofibrillar protein.

Analysis of SDS-PAGE results

Three main MPs bands were found: myosin heavy chain (MHC, 220 kDa), paramyosin (100 kDa), and actin (45 kDa) (Fig. 3e). After repeated freeze–thaw cycles, the band intensities of MHC, paramyosin, and actin in cooked crayfish were significantly lower than that in CK, and the bands gradually disappeared as the number of freeze-thaw cycles increased. SDS-PAGE results revealed that MPs were partially degraded or denatured during repeated freeze-thaw cycles, and that the protein degradation or denaturation was getting more pronounced. The result was consistent with the TBARS and TVB-N values and demonstrated the oxidative degradation of MPs in cooked crayfish. In the same way, Ali et al. (2015) has reported that the intensities of the bands between 130 and 86 kDa decreased inconsistently as the number of freeze-thaw cycles increased in the MPs of chicken breast. The observation suggested that frozen storage may lead to proteolytic degradation or digestion of MPs.

Analysis of SEM results

The microstructure of cooked crayfish is related to its texture, WHC, and other quality properties. It may be seen in Fig. 4 that the microstructure of the cooked crayfish without repeated freeze-thaw cycles was continuous, uniform, and dense, while the microstructure of the cooked crayfish after repeated freeze-thaw cycles was irregular, rough, and had large aggregates. The microstructure of the muscle fibers was destroyed and was manifested by the enlargement of the muscle fiber gap. The above results indicated that the damage to the structure of cooked crayfish muscle fibers

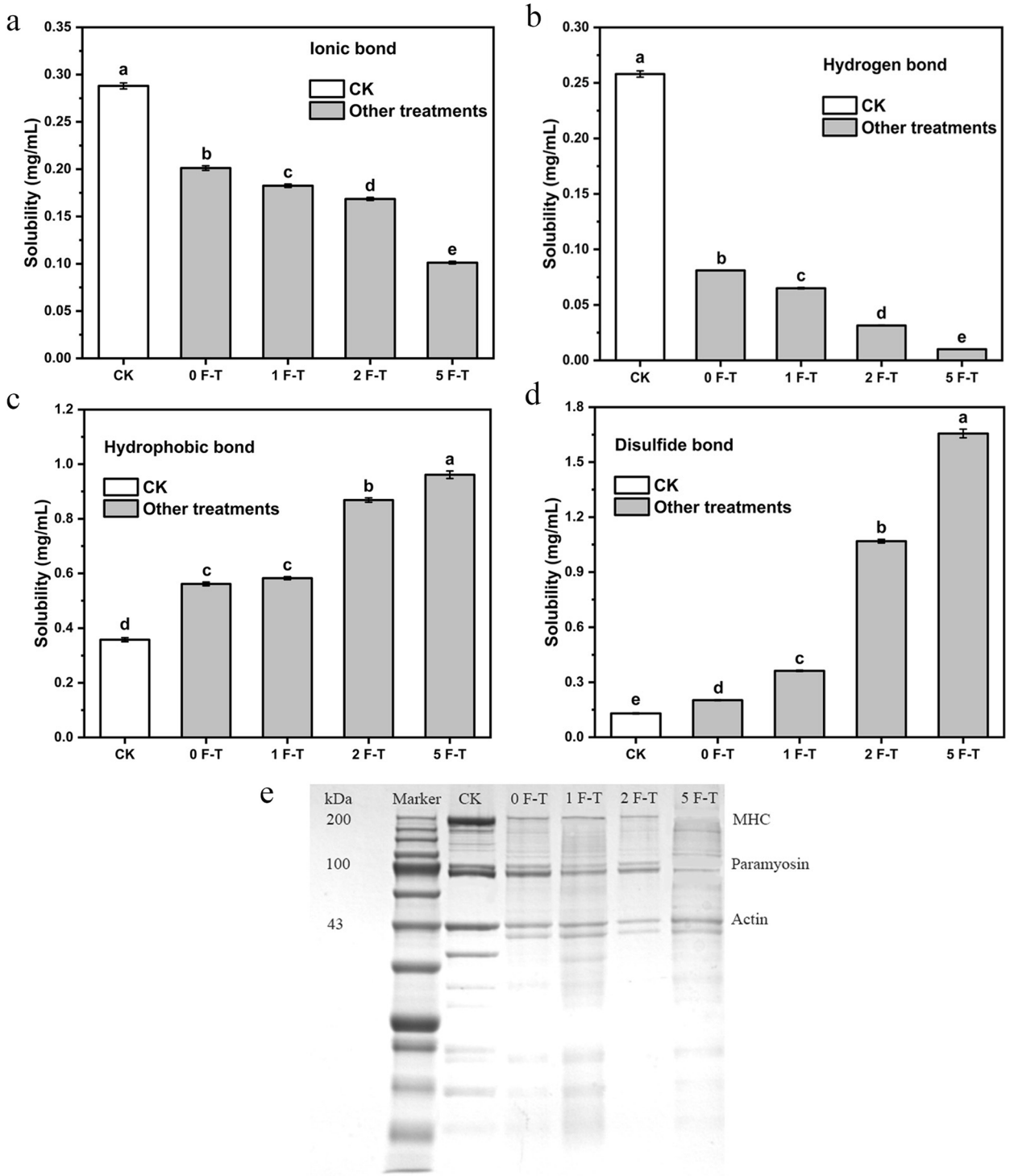

Fig. 3 Effect of repeated freeze-thaw cycles on the chemical forces in cooked crayfish (**a**–**d**) and SDS-PAGE patterns of MPs of cooked crayfish with repeated freeze-thaw cycles (**e**) (CK: fresh crayfish; 0 F-T: cooked crayfish with 0 freeze-thaw cycles; 1 F-T: cooked crayfish with 1 freeze-thaw cycle; 2 F-T: cooked crayfish with 2 freeze-thaw cycles; 5 F-T: cooked crayfish with 5 freeze-thaw cycles). Different letters in the same column of the same indicator showed significant difference ($p < 0.05$)

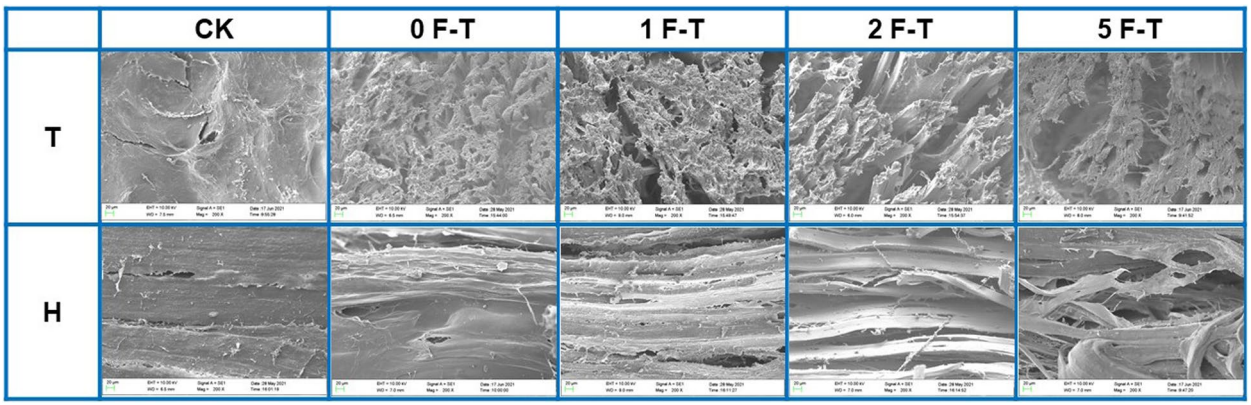

Fig. 4 Effect of repeated freeze-thaw cycles on the microstructure of cooked crayfish (T: transverse direction; L: longitudinal direction) (CK: fresh crayfish; 0 F-T: cooked crayfish with 0 freeze-thaw cycle; 1 F-T: cooked crayfish with 1 freeze-thaw cycle, 2 F-T: cooked crayfish with 2 freeze-thaw cycles, 5 F-T: cooked crayfish with 5 freeze-thaw cycles)

with the increasing number of freeze-thaw cycles, which may be related to the degradation of MPs and the mechanical damage caused by the ice crystals during repeated freeze-thaw process. Wang et al. (2021) found that ice crystals formed repeatedly during the freeze-thaw cycles are likely to cause mechanical damage to the muscle fibers causing their breakage. A similar observation was seen in the study by Sun, Sun, et al. (2019), in which there was a disruption in the intact meat loaf tissue structure due to the formation of numerous ice crystals inside and outside the cells after repeated freeze-thaw cycles.

Pearson correlation analysis of physicochemical properties on the quality of cooked crayfish

The relationship between physicochemical properties and quality can be further illustrated by correlation analyses. The Pearson correlation analysis was performed in this work (Fig. 5). The results demonstrated that some indicators showed significant positive and negative correlations: the value of WHC ($r=0.9981$) was positively correlated with pH, the value of TVB-N ($r=0.9944$) and the solubility of the disulfide bond ($r=0.9921$) were positively correlated with the value of TBARS, and the

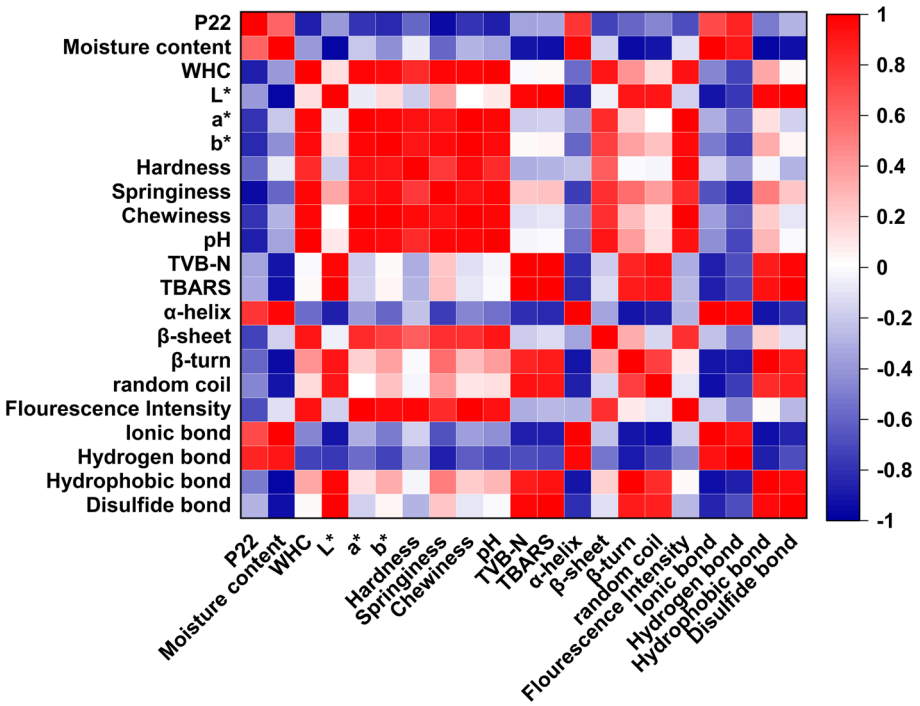

Fig. 5 Pearson correlations of physicochemical properties and structure on cooked crayfish (P_{22}: percentage of T_{22})

content of α-helix ($r = 0.9913$) was positively correlated with the solubility of the ionic bond. The results were consistent with the results of the aforementioned studies. The literature indicated that the loss of WHC may accelerate protein denaturation in biochemical reactions, particularly, oxidation in shrimp (Laorenza & Harnkarnsujarit 2021).

Conclusion

In conclusion, repeated freeze–thaw cycles led to changes in the physicochemical properties and structures of cooked crayfish by exacerbating water loss and destroying the structure of the MPs. More specifically, the repeated freeze-thaw cycles reduced the WHC, moisture content and pH of cooked crayfish, and increased its DL and total color difference ($p < 0.05$). Meanwhile, the repeated freeze-thaw cycles intensified the lipid and protein oxidation. SDS-PAGE maps revealed the partial degradation or denaturation of the MPs due to intensification of lipid and protein oxidation. Raman and UV spectra indicated destabilization of the secondary and tertiary structures of MPs. In addition, changes in the chemical force also demonstrated changes in the structure of the MPs. SEM results showed that after repeated freeze-thaw cycles, the microstructure of cooked crayfish was disrupted and that the tissue structure was no longer intact. Therefore, repeated freeze-thaw cycles deteriorated the color and texture properties (hardness, springiness, and chewiness) of cooked crayfish. This study explored the mechanism by which freeze-thaw cycling can damage cooked crayfish in frozen storage. The results implied that the damage caused by freeze-thaw cycles can be mitigated by maintaining the structural integrity of the proteins and high moisture content.

Acknowledgements
The authors are thankful to the support from the Jiangsu Agricultural Science and Technology Innovation Fund [CX(21)2030] and Basic Scientific Research Project of Jiangsu Academy of Agricultural Sciences [ZX(22)5004]. We thank LetPub (www.letpub.com) for its linguistic assistance during the preparation of this manuscript.

Authors' contributions
J. Han - Acquisition, analysis, interpretation of data, and writing the original draft with the assistance of Y. Sun; N. Jiang - conceptualization and design of the work; R. Sun - substantially revised it; T. Zhang - data analysis; C. Wang - formal analysis. The authors read and approved the final manuscript.

Funding
This work was supported by the Jiangsu Agricultural Science and Technology Innovation Fund (CX(21)2030) and the Basic Scientific Research Project of Jiangsu Academy of Agricultural Sciences (ZX(22)5004).

Availability of data and materials
The datasets used and/or analysed during the current study are available from the corresponding author on reasonable request.

Declarations

Ethics approval and consent to participate
Not applicable.

Consent for publication
Not applicable.

Competing interests
The authors declare that they have no competing interests.

Author details
[1]Institute of Farm Product Processing, Jiangsu Academy of Agricultural Sciences, Nanjing 210014, People's Republic of China. [2]College of Food and Bioengineering, Jiangsu University, Zhenjiang 212013, People's Republic of China. [3]Integrated Scientific Research Base for Preservation, Storage and Processing Technology of Aquatic Products of the Ministry of Agriculture and Rural Areas, Nanjing, People's Republic of China. [4]College of Food Science and Engineering, Nanjing University of Finance & Economics, Nanjing 210014, People's Republic of China.

Received: 4 July 2022 Accepted: 1 September 2022
Published online: 05 October 2022

References

Alarcon-Rojo, A. D., Carrillo-Lopez, L. M., Reyes-Villagrana, R., Huerta-Jiménez, M., & Garcia-Galicia, I. A. (2019). Ultrasound and meat quality: A review. *Ultrasonics Sonochemistry*, *55*, 369–382. https://doi.org/10.1016/j.ultsonch.2018.09.016.

Ali, S., Zhang, W., Rajput, N., Khan, M. A., Li, C. B., & Zhou, G. H. (2015). Effect of multiple freeze-thaw cycles on the quality of chicken breast meat. *Food Chemistry*, *173*, 808–814. https://doi.org/10.1016/j.foodchem.2014.09.095.

Alizadeh-Sani, M., Tavassoli, M., Mohammadian, E., Ehsani, A., Khaniki, G. J., Priyadarshi, R., & Rhim, J.-W. (2021). pH-responsive color indicator films based on methylcellulose/chitosan nanofiber and barberry anthocyanins for real-time monitoring of meat freshness. *International Journal of Biological Macromolecules*, *166*, 741–750. https://doi.org/10.1016/j.ijbiomac.2020.10.231.

Chen, B., Zhou, K., Wang, Y., Xie, Y., Wang, Z., Li, P., & Xu, B. (2020). Insight into the mechanism of textural deterioration of myofibrillar protein gels at high temperature conditions. *Food Chemistry*, *330*. https://doi.org/10.1016/j.foodchem.2020.127186.

Chen, Y., Li, M., Dharmasiri, T. S. K., Song, X., Liu, F., & Wang, X. (2020). Novel ultrasonic-assisted vacuum drying technique for dehydrating garlic slices and predicting the quality properties by low field nuclear magnetic resonance. *Food Chemistry*, *306*. https://doi.org/10.1016/j.foodchem.2019.125625.

Dean, R. T., Fu, S. L., Stocker, R., & Davies, M. J. (1997). Davies biochemistry and pathology of radical mediated protein oxidation. biochem j. *Biochemical Journal, 324* (1), 1–18.

Du, X., Li, H., Dong, C., Ren, Y., Pan, N., Kong, B., … Xia, X. (2021). Effect of ice structuring protein on the microstructure and myofibrillar protein structure of mirror carp (Cyprinus carpio L.) induced by freeze-thaw processes. *LWT*, *139*, 110570. https://doi.org/10.1016/j.lwt.2020.110570.

Duan, X., Li, J., Zhang, Q., Zhao, T., Li, M., Xu, X., & Liu, X. (2017). Effect of a multiple freeze-thaw process on structural and foaming properties of individual egg white proteins. *Food Chemistry*, *228*, 243–248. https://doi.org/10.1016/j.foodchem.2017.02.005.

Felix, M., Romero, A., Rustad, T., & Guerrero, A. (2017). Physicochemical, microstructure and bioactive characterization of gels made from crayfish protein. *Food Hydrocolloids*, *63*, 429–436. https://doi.org/10.1016/j.foodhyd.2016.09.025.

Frelka, J. C., Phinney, D. M., Yang, X. Y., Knopp, M. V., Heldman, D. R., Wick, M. P., & Vodovotz, Y. (2019). Assessment of chicken breast meat quality after freeze/thaw abuse using magnetic resonance imaging techniques. *Journal of the Science of Food and Agriculture*, *99*(2), 844–853. https://doi.org/10.1002/jsfa.9254.

Guo, F.-X., Xiong, Y. L., Qin, F., Jian, H.-J., Huang, X.-L., & Chen, J. (2015). Examination of the causes of instability of soy protein isolate during storage through probing of the heat-induced aggregation. *Journal of the American Oil Chemists' Society*, *92*(8), 1075–1084. https://doi.org/10.1007/s11746-015-2684-6.

Hu, F., Qian, S., Huang, F., Han, D., Li, X., & Zhang, C. (2021). Combined impacts of low voltage electrostatic field and high humidity assisted-thawing on quality of pork steaks. *LWT*, *150*, 111987. https://doi.org/10.1016/j.lwt.2021.111987.

Hu, Y., Zhang, L., Yi, Y., Solangi, I., Zan, L., & Zhu, J. (2021). Effects of sodium hexametaphosphate, sodium tripolyphosphate and sodium pyrophosphate on the ultrastructure of beef myofibrillar proteins investigated with atomic force microscopy. *Food Chemistry*, *338*. https://doi.org/10.1016/j.foodchem.2020.128146.

Jiang, Q., Nakazawa, N., Hu, Y., Osako, K., & Okazaki, E. (2019). Changes in quality properties and tissue histology of lightly salted tuna meat subjected to multiple freeze-thaw cycles. *Food Chemistry*, *293*, 178–186. https://doi.org/10.1016/j.foodchem.2019.04.091.

Lan, M., Li, L., Peng, X., Chen, J., Cao, Q., He, N., … Zhang, X. (2021). Effects of different lipids on the physicochemical properties and microstructure of pale, soft and exudative (PSE)-like chicken meat gel. *Lwt-Food Science and Technology*, *145*. https://doi.org/10.1016/j.lwt.2021.111284.

Lan, W., Hu, X., Sun, X., Zhang, X., & Xie, J. (2020). Effect of the number of freeze-thaw cycles number on the quality of Pacific white shrimp (Litopenaeus vannamei): An emphasis on moisture migration and microstructure by LF-NMR and SEM. *Aquaculture and Fisheries*, *5*(4), 193–200. https://doi.org/10.1016/j.aaf.2019.05.007.

Laorenza, Y., & Harnkarnsujarit, N. (2021). Carvacrol, citral and α-terpineol essential oil incorporated biodegradable films for functional active packaging of Pacific white shrimp. *Food Chemistry*, *363*, 130252. https://doi.org/10.1016/j.foodchem.2021.130252.

Leygonie, C., Britz, T. J., & Hoffman, L. C. (2012). Impact of freezing and thawing on the quality of meat: Review. *Meat Science*, *91*(2), 93–98. https://doi.org/10.1016/j.meatsci.2012.01.013.

Li, F., Zhong, Q., Kong, B., Wang, B., Pan, N., & Xia, X. (2020). Deterioration in quality of quick-frozen pork patties induced by changes in protein structure and lipid and protein oxidation during frozen storage. *Food Research International*, *133*, 109142. https://doi.org/10.1016/j.foodres.2020.109142.

Li, J., Shi, J., Huang, X., Zou, X., Li, Z., Zhang, D., … Xu, Y. (2020). Effects of pulsed electric field on freeze-thaw quality of Atlantic salmon. *Innovative Food Science & Emerging Technologies*, *65*. https://doi.org/10.1016/j.ifset.2020.102454.

Li, J., Wang, J., Zhai, J., Gu, L., Su, Y., Chang, C., & Yang, Y. (2021). Improving gelling properties of diluted whole hen eggs with sodium chloride and sodium tripolyphosphate: Study on intermolecular forces, water state and microstructure. *Food Chemistry*, *358*. https://doi.org/10.1016/j.foodchem.2021.129823.

Li, Y., Tang, X., Shen, Z., & Dong, J. (2019). Prediction of total volatile basic nitrogen (TVB-N) content of chilled beef for freshness evaluation by using viscoelasticity based on airflow and laser technique. *Food Chemistry*, *287*, 126–132. https://doi.org/10.1016/j.foodchem.2019.01.213.

Pan, C., Liang, X., Chen, S., Tao, F., Yang, X., & Cen, J. (2020). Red color-related proteins from the shell of red swamp crayfish (Procambarus clarkii): Isolation, identification and bioinformatic analysis. *Food Chemistry*, *327*. https://doi.org/10.1016/j.foodchem.2020.127079.

Pan, N., Hu, Y., Li, Y., Ren, Y., Kong, B., & Xia, X. (2021). Changes in the thermal stability and structure of myofibrillar protein from quick-frozen pork patties with different fat addition under freeze-thaw cycles. *Meat Science*, *175*. https://doi.org/10.1016/j.meatsci.2020.108420.

Shi, H., Zhou, T., Wang, X., Zou, Y., Wang, D., & Xu, W. (2021). Effects of the structure and gel properties of myofibrillar protein on chicken breast quality treated with ultrasound-assisted potassium alginate. *Food Chemistry*, *358*. https://doi.org/10.1016/j.foodchem.2021.129873.

Shi, L., Xiong, G., Yin, T., Ding, A., Li, X., Wu, W., … Wang, L. (2020). Effects of ultra-high pressure treatment on the protein denaturation and water properties of red swamp crayfish (*Procambarus clarkia*). *LWT*, *133*, 110124. https://doi.org/10.1016/j.lwt.2020.110124.

Sinha, A., & Bhargav, A. (2020). Effect of state transition, drying kinetics and moisture content on Young's modulus variation during thermal drying of hygroscopic food materials. *Journal of Food Engineering*, *279*. https://doi.org/10.1016/j.jfoodeng.2020.109957.

Sun, Q., Chen, Q., Xia, X., Kong, B., & Diao, X. (2019). Effects of ultrasound-assisted freezing at different power levels on the structure and thermal stability of common carp (*Cyprinus carpio*) proteins. *Ultrasonics Sonochemistry*, *54*, 311–320. https://doi.org/10.1016/j.ultsonch.2019.01.026.

Sun, Q., Kong, B., Liu, S., Zheng, O., & Zhang, C. (2021). Ultrasound-assisted thawing accelerates the thawing of common carp (*Cyprinus carpio*) and improves its muscle quality. *Lwt-Food Science and Technology*, *141*. https://doi.org/10.1016/j.lwt.2021.111080.

Sun, Q., Sun, F., Xia, X., Xu, H., & Kong, B. (2019). The comparison of ultrasound-assisted immersion freezing, air freezing and immersion freezing on the muscle quality and physicochemical properties of common carp (Cyprinus carpio) during freezing storage. *Ultrasonics Sonochemistry*, *51*, 281–291. https://doi.org/10.1016/j.ultsonch.2018.10.006.

Tan, M., Lin, Z., Zu, Y., Zhu, B., & Cheng, S. (2018). Effect of multiple freeze-thaw cycles on the quality of instant sea cucumber: Emphatically on water status of by LF-NMR and MRI. *Food Research International*, *109*, 65–71. https://doi.org/10.1016/j.foodres.2018.04.029.

Wachirasiri, K., Wanlapa, S., Uttapap, D., Puttanlek, C., & Rungsardthong, V. (2019). Effects of Multiple Freeze–Thaw Cycles on Biochemical and Physical Quality Changes of White Shrimp (*Penaeus vannamei*) Treated with Lysine and Sodium Bicarbonate. *Journal of Food Science*, *84*(7), 1784–1790. https://doi.org/10.1111/1750-3841.14635.

Wang, B., Du, X., Kong, B., Liu, Q., Li, F., Pan, N., … Zhang, D. (2020). Effect of ultrasound thawing, vacuum thawing, and microwave thawing on gelling properties of protein from porcine longissimus dorsi. *Ultrasonics Sonochemistry*, *64*, 104860. https://doi.org/10.1016/j.ultsonch.2019.104860.

Wang, B., Li, F., Pan, N., Kong, B., & Xia, X. (2021). Effect of ice structuring protein on the quality of quick-frozen patties subjected to multiple freeze-thaw cycles. *Meat Science*, *172*. https://doi.org/10.1016/j.meatsci.2020.108335.

Wang, R., Zhang, L., Chi, Y., & Chi, Y. (2022). Forces involved in freeze-induced egg yolk gelation: Effects of various bond dissociation reagents on gel properties and protein structure changes. *Food Chemistry*, *371*, 131190. https://doi.org/10.1016/j.foodchem.2021.131190.

Xu, Q., Peng, X., Guo, H., Che, Y., Dou, Z., Xing, Z., … Zhang, H. (2022). Rice-crayfish coculture delivers more nutrition at a lower environmental cost. *Sustainable Production and Consumption*, *29*, 14–24. https://doi.org/10.1016/j.spc.2021.09.020.

Xu, Y., Xiao, Y., Lagnika, C., Li, D., Liu, C., Jiang, N., … Zhang, M. (2020). A comparative evaluation of nutritional properties, antioxidant capacity and physical characteristics of cabbage (Brassica oleracea var. capitate var L.) subjected to different drying methods. *Food Chemistry*, *309*. https://doi.org/10.1016/j.foodchem.2019.06.002.

Yang, H., Tao, F., Cao, G., Han, M., Xu, X., Zhou, G., & Shen, Q. (2021). Stability improvement of reduced-fat reduced-salt meat batter through modulation of secondary and tertiary protein structures by means of high pressure processing. *Meat Science*, *176*. https://doi.org/10.1016/j.meatsci.2021.108439.

Zhou, K., Zhang, J., Xie, Y., Wang, Z., Wu, X., Li, C., … Xu, B. (2021). Hemin from porcine blood effectively stabilized color appearance and odor of prepared pork chops upon repeated freeze-thaw cycles. *Meat Science*, *175*, 108432. https://doi.org/10.1016/j.meatsci.2021.108432.

Zhuang, X., Wang, L., Jiang, X., Chen, Y., & Zhou, G. (2021). Insight into the mechanism of myofibrillar protein gel influenced by konjac glucomannan: Moisture stability and phase separation behavior. *Food Chemistry*, *339*. https://doi.org/10.1016/j.foodchem.2020.127941.

Publisher's Note